Polymer Chemistry

ROYAL SOCIETY OF CHEMISTRY

PAPER

View Article Online
View Journal | View Issue

Cite this: *Polym. Chem.*, 2022, **13**, 2340

Next generation strategy for tuning the thermoresponsive properties of micellar and hydrogel drug delivery vehicles using ionic liquids†

Talia A. Shmool, ‡[a] Anna P. Constantinou, ‡[b] Andreas Jirkas, [a] Chen Zhao, [b] Theoni K. Georgiou [b] and Jason P. Hallett *[a]

Amongst the greatest challenges in developing injectable controlled thermoresponsive micellar and hydrogel drug delivery vehicles include tuning the cloud point (CP) and reducing the gelation temperature (T_{gel}), below 37 °C, without compromising stability and solubility. Here, a unique strategy is employed using ionic liquid (IL) matrices to produce stable micellar and hydrogel delivery vehicles of distinct thermoresponsive properties. Each formulation includes the in-house synthesised polymer OEGMA300$_{20}$-*b*-BuMA$_{22}$-*b*-DEGMA$_{11}$ with FITC-IgG. Both micellar-IL and hydrogel-IL formulations exhibit enhanced stability following 120 days of storage under 4 °C compared to in phosphate buffered saline (PBS). Visual tests demonstrate that the CP of the micellar-IL carriers can be finely tuned (31–46 °C). Rheology measurements show that hydrogel strength is significantly increased and T_{gel} is reduced from 40 °C in PBS to 30 °C with IL. Finally, a unique stabilisation mechanism is proposed, triggered by the synergetic action of the excipients and IL in each system.

Received 13th January 2022,
Accepted 16th March 2022

DOI: 10.1039/d2py00053a

rsc.li/polymers

Introduction

Thermoresponsive polymers have attracted increasing interest, with applications in targeted and sustained release vaccines and as topical and injectable scaffolds.[1–3] This promising class of smart drug delivery vehicles includes hydrogels, micelles, interpenetrating networks and nanoparticles.[2–4] Advantageously, physical hydrogels can present thermoreversible gelation properties in aqueous solutions, from room temperature to body temperature, serving as injectable drug delivery vehicles.[3–6] Similarly, thermoresponsive polymeric micelles can show variable cloud points (CP), valuable for targeted and controlled drug delivery.[7–11] Thus, as opposed to acting passively as traditional drug carriers, thermoresponsive polymers can interact and respond to environmental stimuli offering great potential for biomedical applications.

Recently, we have discovered a family of thermoresponsive ABC triblock terpolymers based on oligo(ethylene glycol) methyl ether methacrylate with average M_n 300 g mol^{-1} (OEGMA300, A block), *n*-butyl methacrylate (BuMA, B block) and di(ethylene glycol) methyl ether methacrylate (DEGMA, C block) (Fig. 1).[12,13] The polymer structure consists of one hydrophobic central block, BuMA, and two hydrophilic outer blocks, OEGMA300 and DEGMA. The DEGMA units exhibit thermoresponsive behaviour at approximately 30 °C, expressed as CP.[13,14] The combination of these three blocks allows micelle self-assembly above the critical micelle concentration (CMC), as OEGMA300 and DEGMA are exposed to water at 25 °C and BuMA forms the micelle core. With increasing temperature DEGMA becomes hydrophobic, promoting elongation of the micelles and forming a stable three-dimensional

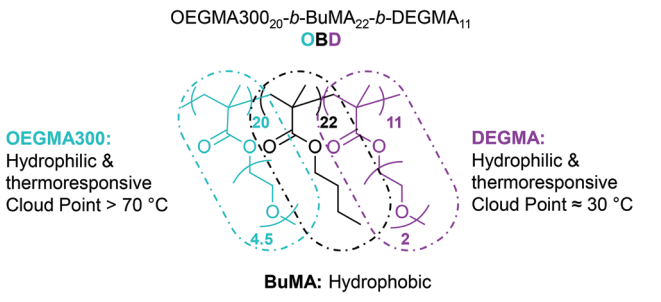

Fig. 1 Chemical structure of the thermoresponsive polymer OEGMA300$_{20}$-*b*-BuMA$_{22}$-*b*-DEGMA$_{11}$ (OBD), with hydrophilic OEGMA300 units shown in cyan, hydrophobic BuMA units in black, and thermoresponsive DEGMA units in purple.

[a]*Department of Chemical Engineering, Imperial College London, South Kensington Campus, London SW7 2AZ, UK. E-mail: j.hallett@imperial.ac.uk; Tel: +44 (0)20 7594 5388*
[b]*Department of Materials, Imperial College London, South Kensington, London SW7 2AZ, UK*

†Electronic supplementary information (ESI) available. See DOI: https://doi.org/10.1039/d2py00053a

‡These authors contributed equally to this work.

network for injectable hydrogel drug delivery applications. Additionally, in concentrated solutions these three units exhibit gelation behaviour, and a member of this family, namely $OEGMA300_{20}$-*b*-$BuMA_{22}$-*b*-$DEGMA_{11}$,(OBD) shows high solubility at 25 °C.[13] Notably, as solution concentration is increased from 10 to 20 w/w% in phosphate buffered saline (PBS), the gelation temperature (T_{gel}) decreases from 44 to 40 °C.[13]

While OBD exhibits high physical and chemical stability in PBS, its T_{gel} of 40 °C at 20 w/w% is outside the biological regime, thus rendering it not suitable for therapeutic applications. Furthermore, above the CMC, at 2 w/w% in PBS, OBD presents a CP of 47 °C, enabling high drug loading, reduced premature drug release and increased bioavailability.[15] However, given the relatively high CP, while sustained drug release is possible, injectable temperature-responsive drug delivery is not feasible. Thus, CP tunability would be highly advantageous, enabling expansion and diversification of OBD applications and of similar thermoresponsive micellar delivery vehicles.

Typically, tailored formulations using different traditional excipients, including sugars, amino acids, polyols and aqueous buffers such as citrate or PBS are developed to tune the properties and enhance the stability of active ingredients and polymeric delivery vehicles in solution.[16,17] However, these excipients can alter the structural stability of biomolecules, leading to irreversible aggregation and degradation.[17,18] As well, the interactions between the polymer and aqueous solvent may change, influencing the hydrophilic/hydrophobic balance of the polymer molecules and hence the thermoresponsive properties.[2,17–19] Furthermore, there remains the hurdle of designing stable drug formulations of extended shelf-life and sustained release.[2,4,15–18] Thus, controlling the thermoresponsive properties of delivery vehicles, whilst maintaining solubility and stability in solution, hinders advancements in drug delivery applications. These challenges are largely due to the lack of delivery vehicles developed, few excipients available, and appropriate matrices established to date for injectable and controlled drug delivery.

Currently, we have developed a strategy using ionic liquids (IL) and traditional excipients, at specific concentrations, to stabilise and control the responsive behaviour of materials upon different external stimuli.[20,21] ILs are composed entirely of cations and anions and form liquids near or below 100 °C.[22] By selecting different ions we can modulate the properties of a system for desired biological applications.[21,23] Given the unique properties of ILs, room-temperature ILs can play a key role in pharmaceutical innovation as a new class of chemical excipients. In the context of drug delivery, ILs can be used to prevent aggregation and precipitation of delivery vehicles and proteins and enhance the solubility, thermal and structural stability of materials in solution.[20–23] In particular, the ILs choline chloride [Cho][Cl], choline dihydrogen phosphate [Cho][DHP] and choline acetate [Cho][OAC] have shown great promise as protein and enzyme stabilisers in aqueous solutions (Fig. 2). Notably, while the mechanism of stabilisation has yet to be completely elucidated,[20–23] these ILs may be useful in the development and stabilisation of antibody conjugated polymeric nanoparticle and hydrogel delivery vehicles for controlled and targeted drug delivery and vaccine applications.

To tackle the ongoing challenges in drug delivery and advance the field of thermoresponsive polymers, for the first time, we combine ILs with traditional excipients to create stable micellar-IL and hydrogel-IL delivery vehicles of controlled CP and T_{gel}, respectively, for injectable drug delivery applications. We also aim to avoid insolubility and aggregation over extended storage. We select the thermoresponsive polymer OBD due to its capability to form well-defined micelles (2 w/w% OBD) or hydrogels (20 w/w% OBD) depending on the concentration used. Our choice of incorporating FITC-IgG as our model protein system is based on its wide use in targeted and controlled drug delivery applications, and to challenge the high aggregation propensity of antibodies in liquid formulations, particularly over extended storage.[17,20,24–29] To design our formulations, we apply our recently developed theoretical and experimental strategy for stabilising active ingredients in solution above 25 °C .[20,21] Here, we use the biocompatible ILs [Cho][Cl], [Cho][DHP] and [Cho][OAC] (Fig. 2) found to effectively stabilise macromaterials in solution mainly *via* hydrogen bonding, hydrophobic and electrostatic interactions.[20,21,23] We produce a series of formulation buffers with different combinations of the traditional excipients, sucrose, trehalose, β-cyclodextrin, L-histidine, L-arginine, tween 20, glycerol, and polyvinylpyrrolidone (PVP). We take into consideration that L-arginine residues can contribute salt bridge interactions,[17,30] and L-histidine and PVP can form a spanning hydrogen bonded network around a protein and with other excipients.[31,32] Additionally, the hydroxyl groups in trehalose, sucrose, cyclodextrin, tween 20 and glycerol could allow for the formation of hydrogen bonds with FITC-IgG surface and OBD. We note that the while the role of these excipients in drug formulations and protein stabilisation has been considerably investigated, the combined effects of the selected excipients with ILs and thermoresponsive polymers has yet to be explored. We challenge our

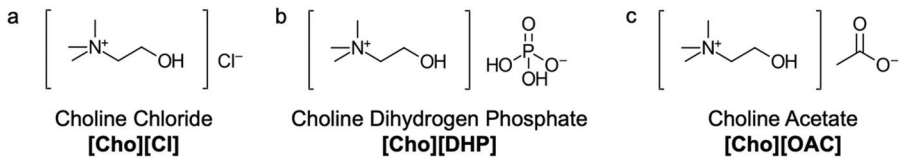

Fig. 2 Chemical structures of (a) choline chloride [Cho][Cl], (b) choline dihydrogen phosphate [Cho][DHP] and (c) choline acetate [Cho][OAC].

approach in that for a given formulation, we selectively produce both stable micellar-IL and hydrogel-IL delivery vehicles, yet of distinct desired thermoresponsive properties. To examine the contribution of the individual ILs, we add [Cho][Cl], [Cho][DHP] and [Cho][OAC] to each prepared buffer and systematically compare the formulations. To characterise our formulations, we obtain the pH and ultraviolet-visible (UV-Vis) spectra of each, and of comparable control systems of FITC-IgG in micellar and hydrogel vehicles in PBS. We conduct zeta potential measurements to determine the charge of each system, and dynamic light scattering (DLS) measurements to compare the size of each sample fresh and following 120 days of storage under 4 °C. Then, we examine the solubility, CP and T_{gel} of each system by visual tests and rheology measurements. Finally, we explore and propose stabilisation and thermoresponsive control mechanisms of the micellar-IL and hydrogel-IL systems developed herein.

Results

IL polymeric delivery vehicle characterisation

Upon addition of OBD to each solution, we observed that for both micellar-IL and hydrogel-IL formulations, containing 2 w/w% and 20 w/w% OBD, respectively, solubility was highest for PBS and [Cho][Cl] formulations, followed by [Cho][OAC] and reduced in the presence of [Cho][DHP].

For each sample, including FITC-IgG in PBS, the absorbance spectra showed characteristic peaks at approximately 300 and 475 nm (Fig. S1†), corresponding to FITC-IgG absorbance in each solution.[25,33–37] This qualitatively indicates that the FITC remained intact, and the IL-delivery vehicles exhibit similar UV absorption spectra to the PBS controls. We note that by DLS and zeta potential measurements we obtained comparable values for FITC-IgG and non-conjugated IgG from human serum in PBS (Tables S1 and S2†), in agreement with the literature.[25,29,37] Thus, we also confirm that FITC conjugation to IgG did not enhance the aggregation propensity of the antibody.

Zeta potential measurements and long-term storage stability study

For both micellar-IL and hydrogel-IL formulations, with pH of approximately 6.5 following adjustment (Table S1†), the zeta potential values remained nearly neutral (ranging from −0.13 ± 0.1 to −5.0 ± 0.1 mV) (Fig. 3a, 4a and Table S1†), as expected based on the chemical composition of OBD.[13] While similar,

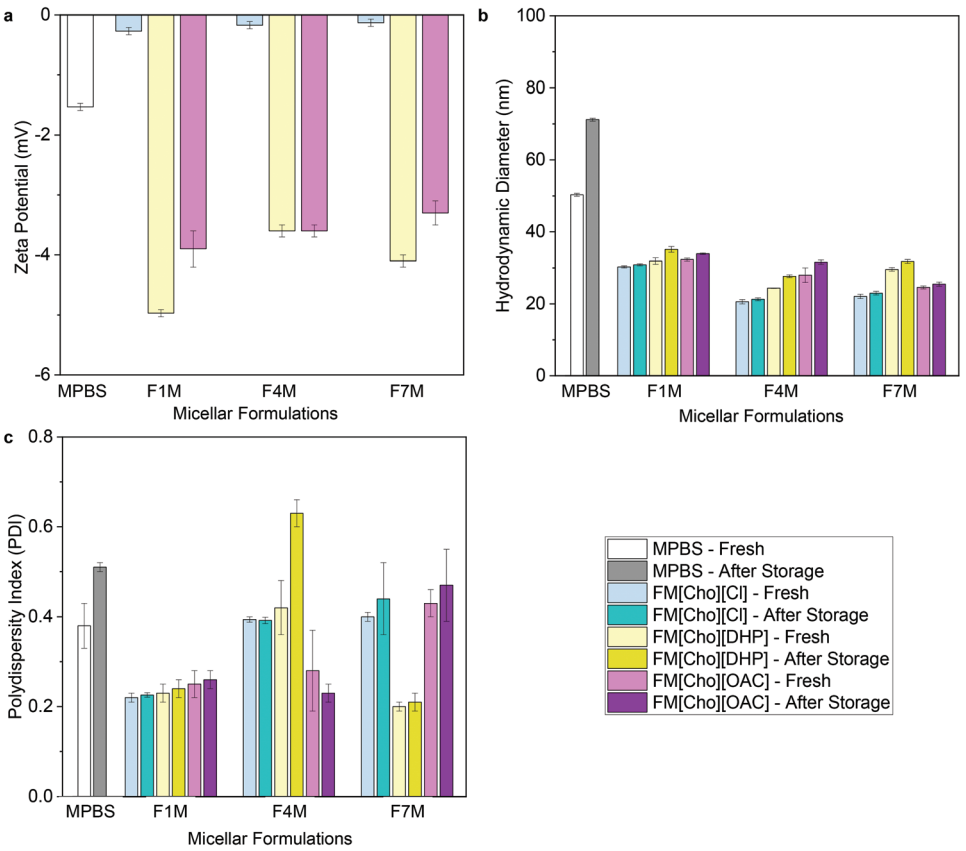

Fig. 3 (a) Zeta-potential values, (b) hydrodynamic diameters, and (c) polydispersity indices of FITC-IgG in micellar-PBS (MPBS) control and select micellar-IL formulations (2 w/w% OBD). Before storage MPBS, FM[Cho][Cl], FM[Cho][DHP], and FM[Cho][OAC] are represented by white, faint blue, faint yellow and magenta, respectively, and after storage by grey, cyan, dark yellow, and purple, respectively. For all micellar-IL formulations see Tables S1 and S3.†

the zeta potential values were slightly lower for FITC-IgG in [Cho][DHP], raised in [Cho][OAC], and highest for [Cho][Cl] formulations, in line with previous work.[20,21,23] Notably, the neutral and minimal difference in zeta potential values compared to the control formulations, FITC-IgG in micellar-PBS (MPBS) (2 w/w% OBD) (−1.5 ± 0.1 mV) and hydrogel-PBS (HPBS) (20 w/w% OBD) (−0.13 ± 0.1 mV), is in agreement with the literature (Table S1†), and also indicates good physical stability of the IL delivery vehicles.[35,36]

To determine the ability of the IL-matrix to protect the antibody from aggregation in solution compared to PBS, we conduct DLS measurements of each sample fresh and following 120 days of storage under 4 °C. Fresh FITC-IgG in the micellar-IL formulations exhibited significantly lower hydrodynamic diameter values (between 20 ± 0.6 nm and 32 ± 0.9 nm) compared to fresh MPBS (50 ± 0.4 nm) (Fig. 3b and Table S3†). Likewise, the fresh hydrogel-IL formulations exhibited significantly lower hydrodynamic diameter values (between 40 ± 0.2 and 48 ± 0.2 nm) compared to fresh FITC-IgG in HPBS (67 ± 0.3) (Fig. 4b and Table S3†). Consistently, IL delivery vehicles showed significantly lower hydrodynamic diameter and polydispersity index (PDI) values compared to micellar and hydrogel delivery vehicles in the absence of IL (Table S4). Additionally, in an attempt to induce aggregation,[29,37] we found that even under stress conditions, following heating of micellar-IL and hydrogel-IL formulations to 60 and 50 °C, respectively, we observed minimal changes in hydrodynamic diameter and PDI values (Table S5†). This further supports our claim of restricted aggregation by the IL delivery vehicles. Following storage, we found that for all IL delivery vehicles particle size was minimally changed, and antibody aggregation was inhibited compared to the control samples (MPBS and HPBS) and delivery vehicles in the absence of IL. Notably, both fresh and following storage, micellar-[Cho][Cl] and hydrogel-[Cho][Cl] vehicles exhibited relatively smaller hydrodynamic diameter and PDI values compared to [Cho][OAC] and [Cho][DHP], also lower in general when combined with β-cyclodextrin, glycerol, or tween 20 (Fig. 3c, 4c and Tables S3, S4†).

Visual tests of micellar-IL delivery vehicles

In examining the ability to tune the CP and properties of the micellar delivery vehicles, Table 1 shows that all micellar-IL formulations exhibited CP values lower than MPBS. Specifically, the micellar-[Cho][DHP] formulations presented

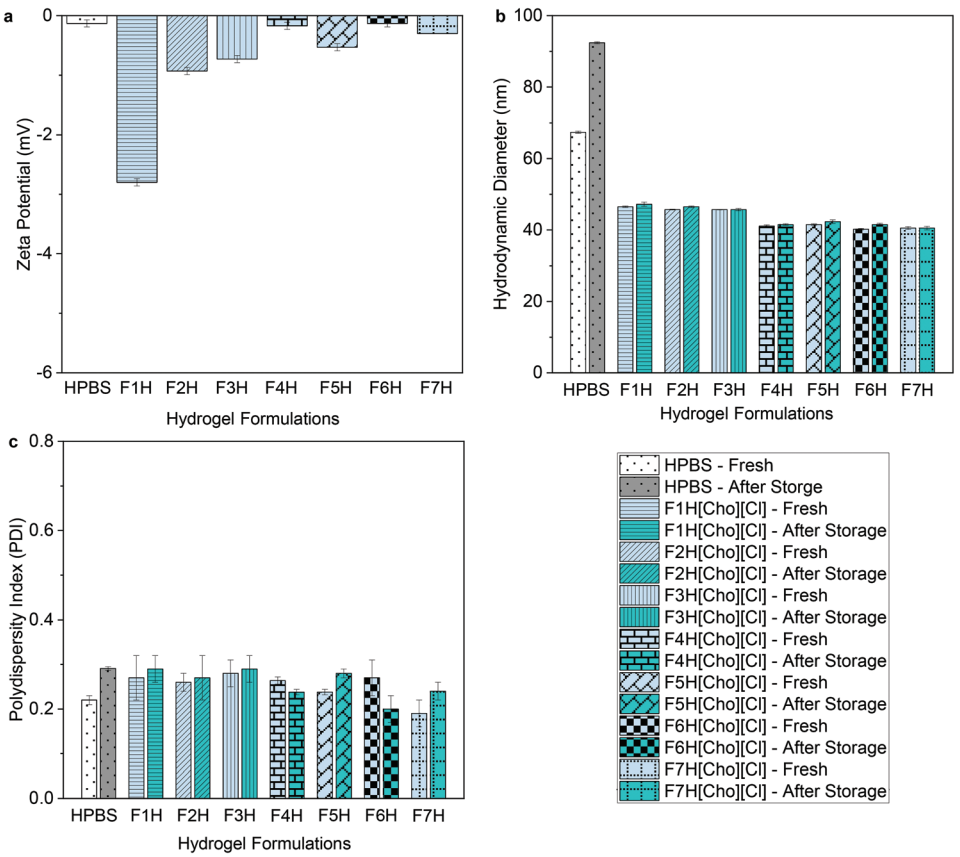

Fig. 4 (a) Zeta-potential values, (b) hydrodynamic diameters, and (c) polydispersity indices for FITC-IgG in hydrogel-PBS (HPBS) control and hydrogel-IL formulations (20 w/w% OBD), before and after storage. Before storage HPBS and the hydrogel-[Cho][Cl] formulations are represented by white and faint blue, respectively; and, after storage by grey and cyan, respectively. To further distinguish, each sample is shaded with a different pattern, including dots (HPBS), horizontal lines (F1H[Cho][Cl]), diagonal lines (F2H[Cho][Cl]), vertical lines (F3H[Cho][Cl]), horizontal bricks (F4H [Cho][Cl]), diagonal bricks (F5H[Cho][Cl]), grey checkerboards (F6H[Cho][Cl]), and dotted grid (F7H[Cho][Cl]).

Table 1 Cloud points of FITC-IgG in the micellar-IL and micellar-PBS (MPBS) (2 w/w% OBD) formulations

Formulation	Cloud points ±2 °C
MPBS	47
F1M[Cho][Cl]	44
F2M[Cho][Cl]	42
F3M[Cho][Cl]	45
F4M[Cho][Cl]	46
F5M[Cho][Cl]	46
F6M[Cho][Cl]	46
F7M[Cho][Cl]	45
F1M[Cho][DHP]	31
F2M[Cho][DHP]	32
F3M[Cho][DHP]	31
F4M[Cho][DHP]	31
F5M[Cho][DHP]	31
F6M[Cho][DHP]	31
F7M[Cho][DHP]	31
F1M[Cho][OAC]	32
F2M[Cho][OAC]	34
F3M[Cho][OAC]	34
F4M[Cho][OAC]	37
F5M[Cho][OAC]	39
F6M[Cho][OAC]	41
F7M[Cho][OAC]	41

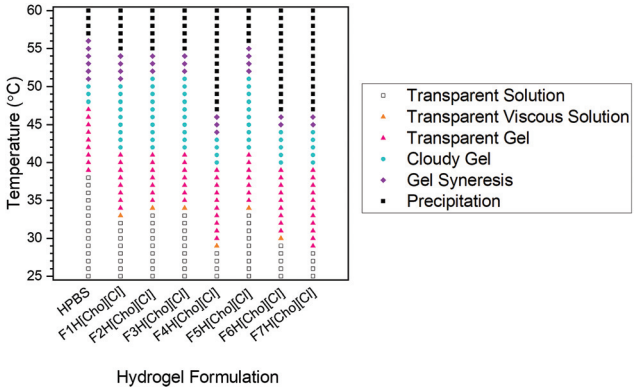

Fig. 5 Visual state of FITC-IgG in HPBS and hydrogel-IL (2 w/w% OBD) formulations, over the temperature range from 25 to 60 °C. White squares correspond to transparent and runny solution, orange triangles indicate transparent viscous solutions. Pink triangles and blue circles indicate transparent and cloudy stable hydrogels; purple diamonds show gel syneresis, and black squares indicate precipitation.

CP values below 37 °C, and [Cho][OAC] formulations exhibited CP values varying between 32 and 41 °C. Most notably, we found that the CP values of micellar-[Cho][Cl] formulations varied from 42 to 46 °C, indicating enhanced thermal stability over a wider higher temperature range, and lower propensity for precipitation.[13] This is also aligned with our observation of improved solubility in micellar-[Cho][Cl] formulations. The manifestation of these properties is attributed to the presence of IL, previously shown to dictate and improve the thermal stability and solubility of proteins in solution.[20,21,23,38]

Taken together with the DLS data, we observe a correlation between the CP and hydrodynamic diameter and PDI values obtained for the micellar-IL delivery vehicles. We found that [Cho][DHP] showed lower CP values and relatively higher particle size, fresh and following storage, compared to [Cho][OAC] and [Cho][Cl]. Overall, these findings demonstrate that along with enabling control and tunability of the CP value, from 31 to 46 °C, our micellar-IL formulations served to protect FITC-IgG from aggregation, fresh and following long-term storage.

Based on the CP values of all the micellar-IL formulations, we highlight that the micellar-[Cho][Cl] carriers exhibited the highest CP values with widest range; and for both micellar-[Cho][Cl] and hydrogel-[Cho][Cl], a nearly neutral charge and smallest change in particle size following storage (Fig. 3, 4 and Tables S1, S3†). Thus, we chose to further study and visually examine all hydrogel-[Cho][Cl] delivery vehicles.

Examining the thermoresponsive properties of hydrogel-IL delivery vehicles

For both HPBS and the hydrogel-IL delivery vehicles, the hydrogels remained stable and no gel syneresis (defined as gel disturbance due to internal stresses)[39,40] was observed up to 43–51 °C (Fig. 5). Upon heating above 48–55 °C, hydrogel syneresis and precipitation (defined as complete phase separation into two phases) was observed for all samples; however, a wider gelation range was detected for the hydrogel-[Cho][Cl] delivery vehicles compared to HPBS. Most notably, in contrast to FITC-IgG in HPBS (20 w/w%), the visual gelation temperature ($T_{gel,V}$) decreased from 39 °C to approximately 29–35 °C, within the biologically relevant regime, highlighting that the IL-excipient matrix serves to reduce $T_{gel,V}$.

Above 25 °C, with increasing temperature, DEGMA becomes hydrophobic, with a transition from hydrophilic to hydrophobic, and the formation of worm-like micelles leads to gelation.[41] As such, we determine the T_{gel} and the strength of the hydrogel-IL delivery vehicles by rheology experiments (Fig. 6). For each sample, we found that at 25 °C the storage modulus (G') was lower than the loss modulus (G''). This indicated that all samples were at liquid state at room temperature. As the temperature was increased, so did the moduli until $G' > G''$, indicating hydrogel formation after which a second crossover followed as the hydrogel destabilised. For each sample, the hydrogel formation temperature obtained from the rheology ($T_{gel,R}$) experiment agreed with the $T_{gel,V}$ value observed by detailed visual tests, within the error of the techniques (Table 2). Additionally, the hydrogel-IL delivery vehicles formed soft hydrogels with maximum storage modulus varying from 120 to 330 Pa. Specifically, F7H[Cho][Cl], containing sucrose, β-cyclodextrin and PVP, formed the strongest hydrogel (G' = 330 Pa) with $T_{gel,R}$ well below body temperature ($T_{gel,R}$ = 31 °C); while F2H[Cho][Cl], containing solely sucrose, showed the highest $T_{gel,R}$ at 36 °C, forming also a weaker hydrogel, G' = 180 Pa. This demonstrates that for each system our IL-matrix strongly controls the T_{gel} value and strength of the hydrogel delivery vehicle, most notably serving to reduce $T_{gel,R}$ by 10 °C (F4H[Cho][Cl], containing trehalose and glycerol) compared to FITC-IgG in HPBS.

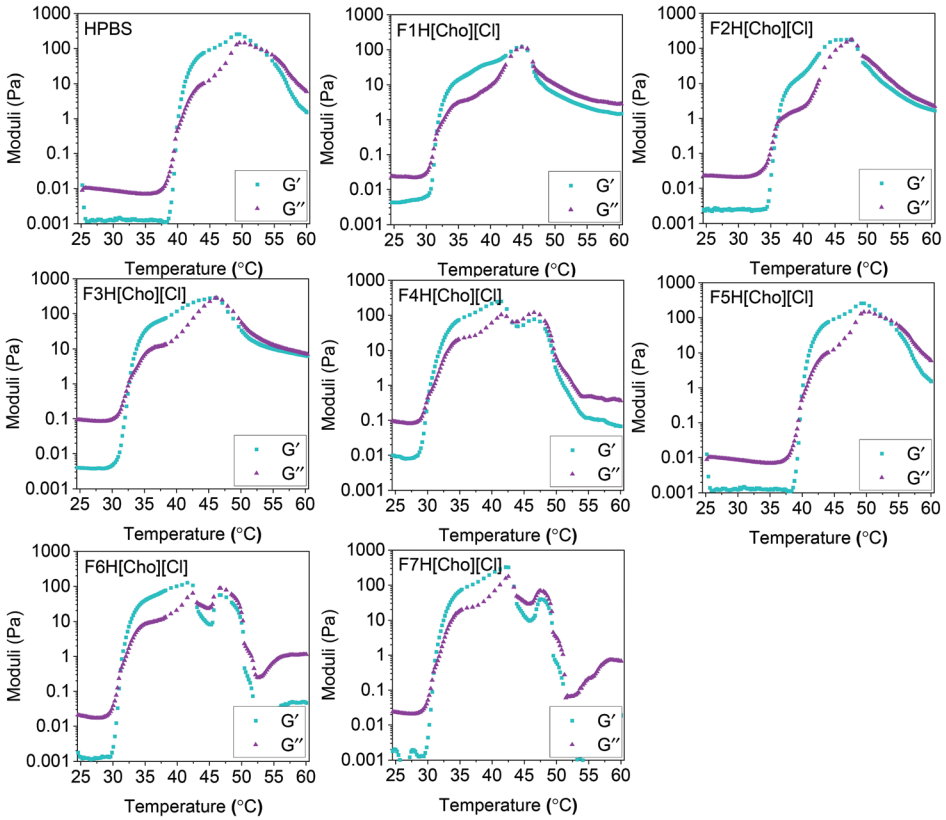

Fig. 6 Storage (G', cyan squares) and loss (G'', purple triangles) moduli as a function of temperature for the hydrogel-IL and HPBS (20 w/w% OBD) formulations.

Table 2 Gelation temperature observed by visual tests ($T_{gel,V}$) and rheology ($T_{gel,R}$) measurements for FITC-IgG in hydrogel-IL and HPBS (20 w/w% OBD) formulations

Hydrogel formulation	$T_{gel,V}$ ±2 °C	$T_{gel,R}$ ±1 °C	Maximum storage modulus (G', Pa)
HPBS	39	40	260
F1H[Cho][Cl]	34	32	120
F2H[Cho][Cl]	35	36	180
F3H[Cho][Cl]	35	33	290
F4H[Cho][Cl]	30	30	250
F5H[Cho][Cl]	35	33	200
F6H[Cho][Cl]	31	31	130
F7H[Cho][Cl]	29	31	330

Discussion

Consistently, for all of our micellar-IL and hydrogel-IL delivery vehicles, the developed IL-matrices reduced particle size and aggregation propensity of FITC-IgG in solution, fresh and following storage, compared to the corresponding control samples, MPBS or HPBS, respectively, and in the absence of IL. Thus, our formulations prove promising for extending the shelf-life of pharmaceuticals. Furthermore, we demonstrate our ability to tune the CP of the thermoresponsive micellar-IL carriers, significant for designing delivery vehicles for controlled drug release. We consider that above the CP, collapse of the micelle structure leads to drug release.[42,43] Specifically, for all micellar-[Cho][DHP] and for micellar-[Cho][OAC] formulations with L-arginine or solely sucrose, the CP temperature was reduced well below body temperature. Given the rapid collapse of the micelles at lower temperatures, these formulations could be suitable for high drug loading and burst drug release.[44] In contrast, for all thermally stable micellar-[Cho][Cl] and for micellar-[Cho][OAC] formulations containing β-cyclodextrin or tween 20, the higher CP observed may allow for enhanced bioavailability and slower drug release, with the delayed micelle collapse enabling diffusion driven drug release.[43]

We rationalise that for the [Cho][Cl] and [Cho][OAC] systems, the increase in electrostatic interactions, hydrogen bond strength and confinement can confer local rigidity and stability to the thermoresponsive polymeric micelles.[45–47] This explains the slightly lower particle sizes in the range of 20–30 nm and also the higher CP temperatures of these formulations. In contrast, for the micellar-[Cho][DHP] formulations, intermolecular hydrogen bonds are likely less abundant due to steric hinderance, as the bulky dihydrogen phosphate chains can prevent a close approach of the hydrogen bond donors and acceptors.[21,23,46–48] Accordingly, the greater steric hinderance and loss in electrostatic repulsions in [Cho][DHP] formulations explains the relatively lower zeta potential values and slight increase in the hydrodynamic diameter values in that

size range. We also note that the presence of hydrophobic alkyl chain, amine group, hydrogen bond accepting carboxylate moiety, and guanidinium functional group can also interact with the protein and polymeric micelles, promoting rearrangement.[17,45,46] This would explain the relatively higher hydrodynamic diameter and PDI values and lower CP values obtained for formulations containing L-arginine.

It has previously been shown that the addition of traditional excipients, including sugars, polyols and surfactants, can increase T_{gel}, reduce gel strength, and result in destabilisation.[49–53] However, when combining such excipients with IL, we observed that in all cases T_{gel} was significantly reduced, and for some formulations mechanical strength was enhanced compared to HPBS. This highlights the role of IL in controlling and tuning the thermoresponsive and mechanical properties of the hydrogels, achieving the desired outcome. We consider that a given hydrogel with T_{gel} higher than body temperature would be unsuitable for sustained injectable drug delivery. Similarly, a hydrogel with T_{gel} and gelation window well below 37 °C would not readily form a gel after injection.[2,5,6] Given that $T_{gel,R}$ of our developed hydrogel-IL formulations ranged between 30 to 36 °C, these show great promise as injectable controlled and targeted drug delivery systems.

Based on our observations from the visual tests, DLS, zeta potential and rheology measurements, we suggest that macromolecular confinement effects strongly regulate $T_{gel,R}$, G', and stability of the hydrogels. Specifically, due to the formation of intricate hydrogen bonding networks, a hydrogel confined within an IL-excipient matrix exhibits significantly altered thermoresponsive properties compared to HPBS, as exemplified by F4H[Cho][Cl], with $T_{gel,R}$ reduced by 10 °C. We note that depending on the mass fraction used in a formulation, glycerol has been shown to act as an antiplasticiser[54,55] and tween 20 can have a plasticising role, enhancing stability.[17,45,56] Given our observations of $T_{gel,R}$ = 30 °C and G' = 250 Pa for F4H[Cho][Cl], we propose that glycerol formed strong hydrogen bonds with the hydroxyl groups of trehalose and [Cho][Cl], thereby increasing the stability of FITC-IgG and the hydrogel in a more rigid matrix. Correspondingly, $T_{gel,R}$ = 33 °C and the lower G' = 200 Pa of F5H[Cho][Cl] implies that the large number of hydroxyl groups present on tween 20 enhance the hydrogen bonding network, maintaining well distributed free volume between the polymer chains, leading to a plasticising effect.[17,44,45,55,56] Furthermore, we found that G' = 330 Pa was highest for F7H[Cho][Cl] indicating high stability, as well as $T_{gel,R}$ = 31 °C. This can be primarily attributed to the formation of hydrogen bonds between β-cyclodextrin, sucrose, PVP and [Cho][Cl] resulting in a more stable amorphous matrix, confining the hydrogel and FITC-IgG and preventing aggregation.[17,20] Accordingly, in the absence of sucrose in F6H[Cho][Cl], a lower degree of confinement by the IL and excipients would result in greater polymer chain flexibility, explaining the significant reduction in G'. This claim is also supported by the higher $T_{gel,R}$ = 36 °C and low G' = 180 Pa observed for F2H[Cho][Cl], further limited in composition to [Cho][Cl] and sucrose. The effect of confinement dictated by the IL-excipient matrix is also highlighted by F1H[Cho][Cl] and F3H[Cho][Cl], each containing IL with sugar and L-arginine at varying amounts. While both show similar $T_{gel,R}$ values, F1H[Cho][Cl] exhibits a significantly lower G' compared to F3H[Cho][Cl] (G' = 120 and 290 Pa, respectively). We consider that despite the expected ability of trehalose to form more and stronger hydrogen bonds with IL and L-arginine compared to sucrose,[57,58] since a lower amount of sugar was used in F1H[Cho][Cl], likely, confinement effects were relatively weak. Thus, the electrostatic, hydrophobic networks and hydrogen bond formation ability of [Cho][Cl] and the excipients provide an important contribution to FITC-IgG and hydrogel stability, and serve to hinder aggregation, lower $T_{gel,R}$, and raise G' compared to traditionally used HPBS.

Conclusions

For both the thermoresponsive micellar-IL and hydrogel-IL delivery vehicles, the negligible change in particle size following 120 days under 4 °C indicates that the IL-matrix stabilised and protected FITC-IgG from aggregation and degradation, encouraging for increasing the shelf-life of pharmaceuticals. The reduced CP values observed for each micellar-[Cho][DHP] and formulations of micellar-[Cho][OAC] with L-arginine or pure sucrose may allow for shorter half-life of a drug in targeted and controlled delivery applications. Conversely, the higher CP observed for each micellar-[Cho][Cl] and select micellar-[Cho][OAC] formulations containing β-cyclodextrin or tween 20 may be suitable for extended drug half-life, thus reducing the frequency of dosing. Our stable hydrogel-IL delivery vehicles showed high solubility, low viscosity and strong mechanical properties, with $T_{gel,R}$ reduced to as low as 30 °C compared to 40 °C in PBS. Notably, the mechanism of gelation and stabilisation did not involve covalent cross-linkers, rather we propose that significant hydrogen bonding, electrostatic and hydrophobic interactions between the IL-excipient matrix and OBD polymer are responsible for the enhanced stability and restricted aggregation. Likely, the alkyl groups of cholinium bind with the protein and OBD polymer *via* hydrophobic interactions, and significant hydrogen bonding and electrostatic interactions between the protein and ILs are also responsible for the enhanced stability. Thus, the difference in behaviour between the thermoresponsive formulations can be attributed to a change in the hydrophilic and hydrophobic balance and confinement effects on these systems by the IL-excipient matrix. Ultimately, these stable injectable drug delivery vehicles are highly promising for targeted and sustained drug release applications.

Materials and methods

Materials

Choline dihydrogen phosphate ([Cho][DHP]) was purchased from abcr GmbH (Karlsruhe, Germany). Choline chloride ([Cho][Cl]), choline acetate ([Cho][OAC]), PBS, sucrose, treha-

lose, β-cyclodextrin, L-histidine/HCl, L-arginine, tween 20, glycerol, PVP, and FITC-IgG and IgG from human serum were purchased from Sigma-Aldrich Company Limited (Gillingham, Dorset, UK), stored as recommended, and used without further purification.

Formulation preparation

As previously described, OBD was synthesised by group transfer polymerisation, purified *via* precipitation, followed by drying in a vacuum oven to evaporate any remaining toxic solvents.[13] Bulk solutions of [Cho][Cl], [Cho][DHP], and [Cho][OAC] at 15 w/w% were prepared as reported prior.[21] Aqueous stock solutions of each buffer, shown in Table 3, were prepared in deionised water at pH 7.4.

Final formulations consisted of 1 : 1.4 : 1.6 (w/w/w%) protein-buffer-IL, with [Cho][Cl], [Cho][DHP] and [Cho][OAC] examined with each buffer. In all cases the total content of OBD in the micellar and hydrogel formulations was 2 w/w% and 20 w/w%, respectively, also in the control samples with PBS. The pH of each solution was measured using the pH electrode Mettler Toledo InLab Micro (WOLFLABS, Pocklington, York, UK) and the average results of three measurements is reported (Table S1†). Based on the obtained pH values (Table S1†), the pH of each formulation was adjusted by addition of L-histidine/HCl to obtain a pH of approximately 6.5. All formulations were prepared, and immediately stored at 4 °C until measured.

Solubility and ultraviolet-visible (UV-Vis) spectroscopy measurements

Following preparation, the solubility of each sample was visually inspected, and each sample was placed in a disposable cuvette (Avantor Inc, Radnor, PA, USA). For each, absorbance was measured using an Agilent Cary UV-Vis Compact Peltier UV-Vis spectrophotometer (Agilent Technologies LDA UK Ltd, Didcot, UK). Scan mode measurements were conducted at 25 °C from 800 to 250 nm at 0.5 nm intervals. For each sample, the corresponding buffer solution was used as a reference.

Dynamic light scattering and zeta potential measurements

To investigate the particle size and polydispersity index (PDI) of each sample, DLS measurements were performed using a Zetasizer Nano ZS (Malvern Panalytical Ltd, Malvern, UK), at a 90° scattering angle, fresh and following four months of storage at 4 °C. 300 μL of each sample was diluted with deionised water at pH 7.4 to a concentration of 0.4 mg mL^{-1}, placed in a disposable cuvette (Brand GmbH, Wertheim, Germany) and allowed to equilibrate to 25 °C for 5 minutes to obtain an appropriate count rate. For each sample, three DLS measurements were conducted with 10 repetitions for each measurement. Hydrodynamic size was determined by applying the Stokes–Einstein equation and average results of the three measurements are reported. Zeta potential measurements were performed using the Litesizer 500 (Anton Paar GmbH, Ostfildern, Germany). The sample, at 0.4 mg mL^{-1}, was placed in an Anton Paar Ω-shaped capillary of the zeta potential cuvette (Anton Paar GmbH, Ostfildern, Germany), and allowed to equilibrate to 25 °C for 5 minutes. For each sample three measurements with 10 runs within each were conducted, with the Smoluchowski approximation applied, and the average results of the measurements are reported.

Visual tests

To conduct visual tests, each sample, prepared in a glass vial (Thermo Fisher Scientific Inc, Waltham, MA, USA), was immersed in a water bath (Philip Harris, Hyde, Cheshire, UK) and continuously stirred using an IKA RCT basic stirrer hotplate (IKA-Werke GmbH, Staufen, Germany). Samples were heated and the temperature was monitored using a temperature controller (Cole Parmer Instrument Company Ltd, St Neots, UK). Samples were observed visually from 25 °C at one-degree intervals. Micelle carriers (2 w/w% OBD) were visually tested to determine the CP, defined as the temperature at which the solution turned from transparent yellow to opaque yellow cloudy. Hydrogel vehicles (20 w/w% OBD) were examined for transitions: transparent and cloudy runny solution, transparent and cloudy viscous solution, transparent and cloudy hydrogel (defined as no flow observed upon tube inversion), gel syneresis, and precipitation.

Rheology experiments

The hydrogel samples were subjected to oscillatory temperature ramp measurements using a TA-Discovery HR-1 hybrid rheometer equipped with a 40 mm Peltier steel plate (TA instruments-Waters LLC, New Castle, DE, USA). A solvent trap

Table 3 Buffer components (w/w%) in each formulation

	Concentration of buffer components (w/w%)							
Buffer	L-Histidine	Trehalose	L-Arginine	Tween 20	Sucrose	Glycerol	β-Cyclodextrin	PVP
F1	0.60	1.8	0.63	—	—	—	—	—
F2	0.15	—	—	—	2.7	—	—	—
F3	0.15	—	0.39	—	2.7	—	—	—
F4	0.29	5.0	—	—	—	0.25	—	—
F5	0.054	5.3	—	0.021	—	—	—	—
F6	0.64	4.2	—	—	—	—	6.7	3.0
F7	0.64	—	—	—	4.2	—	6.7	3.0

(TA instruments-Waters LLC, New Castle, DE, USA) was used during the measurements to prevent solvent evaporation. The angular frequency (ω) and the strain (γ) were kept constant at 1 rad s^{-1} and 1%, respectively. The shear storage and shear loss moduli (G' and G'', respectively) were recorded and T_{gel} was determined, defined as the temperature at which the storage modulus exceeds the loss modulus.

Data availability

All data needed to evaluate the conclusions in the paper are present in the main paper and/or the ESI.† Additional data related to the paper may be requested from the authors.

Author contributions

T. A. S. conceived the project and designed the formulations. T. A. S. and A. J. prepared the formulations, and performed the pH, DLS, and zeta potential measurements. A. P. C. synthesised the polymer, and with C. Z. examined the solubility, conducted UV-Vis spectroscopy measurements, visual tests, and rheology experiments. T. A. S. and A. P. C. analysed the data, wrote the paper, and prepared the ESI.† J. P. H. and T. K. G. supervised the research and provided comments. All authors approved the manuscript.

Conflicts of interest

T. A. Shmool and J. P. Hallett, UK Pat., 2108009.8, 2021. T. K. Georgiou and A. P. Constantinou, PCT/GB2019/052686, 2020. The other authors have no conflicts to declare.

Acknowledgements

This research is funded by the Department of Health and Social Care using UK Aid funding and is managed by the Engineering and Physical Sciences Research Council (EPSRC, grant number: EP/R013764/1). The views expressed in this publication are those of the author(s) and not necessarily those of the Department of Health and Social Care. A. P. C. acknowledges support from the Department of Materials at Imperial College London, the EPSRC Doctoral Prize Fellowship (EP/M506345/1), and the EPSRC Impact Acceleration Grant (EP/R511547/1).

References

1 G. A. Roth, E. C. Gale, M. Alcántara-Hernández, W. Luo, E. Axpe, R. Verma, Q. Yin, A. C. Yu, H. Lopez Hernandez, C. L. Maikawa, A. A. A. Smith, M. M. Davis, B. Pulendran, J. Idoyaga and E. A. Appel, Injectable Hydrogels for Sustained Codelivery of Subunit Vaccines Enhance Humoral Immunity, *ACS Cent. Sci.*, 2020, **6**(10), 1800–1812, DOI: **10.1021/acscentsci.0c00732**.

2 J. Li and D. J. Mooney, Designing Hydrogels for Controlled Drug Delivery, *Nat. Rev. Mater.*, 2016, **1**(12), 16071, DOI: **10.1038/natrevmats.2016.71**.

3 K. Zhang, K. Xue and X. J. Loh, Thermo-Responsive Hydrogels: From Recent Progress to Biomedical Applications, *Gels*, 2021, **7**(3), 77, DOI: **10.3390/gels7030077**.

4 H. Priya James, J. Rijo, A. Anju and K. R. Anoop, Smart Polymers for the Controlled Delivery of Drugs – A Concise Overview, *Acta Pharm. Sin. B*, 2014, **4**(2), 120–127, DOI: **10.1016/j.apsb.2014.02.005**.

5 H. Huang, X. Qi, Y. Chen and Z. Wu, Thermo-Sensitive Hydrogels for Delivering Biotherapeutic Molecules: A Review, *Saudi Pharm. J.*, 2019, **27**(7), 990–999, DOI: **10.1016/j.jsps.2019.08.001**.

6 A. P. Constantinou and T. K. Georgiou, Pre-Clinical and Clinical Applications of Thermoreversible Hydrogels in Biomedical Engineering: A Review, *Polym. Int.*, 2021, **70**(10), 1433–1448, DOI: **10.1002/pi.6266**.

7 H. Wei, X.-Z. Zhang, Y. Zhou, S.-X. Cheng and R.-X. Zhuo, Self-Assembled Thermoresponsive Micelles of Poly (N-Isopropylacrylamide-b-Methyl Methacrylate), *Biomaterials*, 2006, **27**(9), 2028–2034, DOI: **10.1016/j.biomaterials.2005.09.028**.

8 J. E. Chung, M. Yokoyama, M. Yamato, T. Aoyagi, Y. Sakurai and T. Okano, Thermo-Responsive Drug Delivery from Polymeric Micelles Constructed Using Block Copolymers of Poly(N-Isopropylacrylamide) and Poly(Butylmethacrylate), *J. Controlled Release*, 1999, **62**(1–2), 115–127, DOI: **10.1016/s0168-3659(99)00029-2**.

9 H. Wei, X.-Z. Zhang, H. Cheng, W.-Q. Chen, S.-X. Cheng and R.-X. Zhuo, Self-Assembled Thermo- and PH Responsive Micelles of Poly(10-Undecenoic Acid-b-N-Isopropylacrylamide) for Drug Delivery, *J. Controlled Release*, 2006, **116**(3), 266–274, DOI: **10.1016/j.jconrel.2006.08.018**.

10 X.-L. Sun, P.-C. Tsai, R. Bhat, E. M. Bonder, B. Michniak-Kohn and A. Pietrangelo, Thermoresponsive Block Copolymer Micelles with Tunable Pyrrolidone-Based Polymer Cores: Structure/Property Correlations and Application as Drug Carriers, *J. Mater. Chem. B*, 2015, **3**(5), 814–823, DOI: **10.1039/C4TB01494D**.

11 I.-S. Kim, Y.-I. Jeong, Y.-H. Lee and S.-H. Kim, Drug Release from Thermo-Responsive Self-Assembled Polymeric Micelles Composed of Cholic Acid and Poly (N-Isopropylacrylamide), *Arch. Pharmacal Res.*, 2000, **23**(4), 367–373, DOI: **10.1007/BF02975449**.

12 A. P. Constantinou, N. Provatakis, Q. Li and T. K. Georgiou, Homopolymer and ABC Triblock Copolymer Mixtures for Thermoresponsive Gel Formulations, *Gels*, 2021, **7**(3), 116, DOI: **10.3390/gels7030116**.

13 A. P. Constantinou, B. Zhan and T. K. Georgiou, Tuning the Gelation of Thermoresponsive Gels Based on Triblock Terpolymers, *Macromolecules*, 2021, **54**(4), 1943–1960, DOI: **10.1021/acs.macromol.0c02533**.

14 J.-F. Lutz, A. Hoth and K. Schade, Design of Oligo(Ethylene Glycol)-Based Thermoresponsive Polymers: An Optimization Study, *Des. Monomers Polym.*, 2009, **12**(4), 343–353, DOI: **10.1163/156855509X448316**.

15 Y. Lu, E. Zhang, J. Yang and Z. Cao, Strategies to Improve Micelle Stability for Drug Delivery, *Nano Res.*, 2018, **11**(10), 4985–4998, DOI: **10.1007/s12274-018-2152-3**.

16 X. M. Cao, Y. Tian, Z. Y. Wang, Y. W. Liu and C. X. Wang, Effects of Protein and Phosphate Buffer Concentrations on Thermal Denaturation of Lysozyme Analyzed by Isoconversional Method, *Bioengineered*, 2016, **7**(4), 235–240, DOI: **10.1080/21655979.2016.1197629**.

17 S. Ohtake, Y. Kita and T. Arakawa, Interactions of Formulation Excipients with Proteins in Solution and in the Dried State, *Adv. Drug Delivery Rev.*, 2011, **63**(13), 1053–1073, DOI: **10.1016/j.addr.2011.06.011**.

18 R. Rajan, S. Ahmed, N. Sharma, N. Kumar, A. Debas and K. Matsumura, Review of the Current State of Protein Aggregation Inhibition from a Materials Chemistry Perspective: Special Focus on Polymeric Materials, *Mater. Adv.*, 2021, **2**(4), 1139–1176, DOI: **10.1039/D0MA00760A**.

19 Y.-H. Kim, I. C. Kwon, Y. H. Bae and S. W. Kim, Saccharide Effect on the Lower Critical Solution Temperature of Thermosensitive Polymers, *Macromolecules*, 1995, **28**(4), 939–944, DOI: **10.1021/ma00108a022**.

20 T. A. Shmool, L. K. Martin, L. Bui-Le, I. Moya-Ramirez, P. Kotidis, R. P. Matthews, G. A. Venter, C. Kontoravdi, K. M. Polizzi and J. P. Hallett, An Experimental Approach Probing the Conformational Transitions and Energy Landscape of Antibodies: A Glimmer of Hope for Reviving Lost Therapeutic Candidates Using Ionic Liquid, *Chem. Sci.*, 2021, **12**(27), 9528–9545, DOI: **10.1039/D1SC02520A**.

21 T. A. Shmool, L. K. Martin, C. J. Clarke, L. Bui-Le, K. M. Polizzi and J. P. Hallett, Exploring Conformational Preferences of Proteins: Ionic Liquid Effects on the Energy Landscape of Avidin, *Chem. Sci.*, 2021, **12**(1), 196–209, DOI: **10.1039/D0SC04991C**.

22 J. P. Hallett and T. Welton, Room-Temperature Ionic Liquids: Solvents for Synthesis and Catalysis. 2, *Chem. Rev.*, 2011, **111**(5), 3508–3576, DOI: **10.1021/cr1003248**.

23 M. Reslan and V. Kayser, Ionic Liquids as Biocompatible Stabilizers of Proteins, *Biophys. Rev.*, 2018, **10**(3), 781–793, DOI: **10.1007/s12551-018-0407-6**.

24 K. Singh, W. Ejaz, K. Dutta and S. Thayumanavan, Antibody Delivery for Intracellular Targets – Emergent Therapeutic Potential, *Bioconjugate Chem.*, 2019, **30**(4), 1028–1041, DOI: **10.1021/acs.bioconjchem.9b00025**.

25 N. Martin, D. Ma, A. Herbet, D. Boquet, F. M. Winnik and C. Tribet, Prevention of Thermally Induced Aggregation of IgG Antibodies by Noncovalent Interaction with Poly(acrylate) Derivatives, *Biomacromolecules*, 2014, **15**(8), 2952–2962, DOI: **10.1021/bm5005756**.

26 S. Wöhl-Bruhn, M. Badar, A. Bertz, B. Tiersch, J. Koetz, H. Menzel, P. P. Mueller and H. Bunjes, Comparison of In Vitro and In Vivo Protein Release from Hydrogel Systems, *J. Controlled Release*, 2012, **162**(1), 127–133, DOI: **10.1016/j.jconrel.2012.05.049**.

27 A. Bertz, S. Wöhl-Bruhn, S. Miethe, B. Tiersch, J. Koetz, M. Hust, H. Bunjes and H. Menzel, Encapsulation of Proteins in Hydrogel Carrier Systems for Controlled Drug Delivery: Influence of Network Structure and Drug Size on Release Rate, *J. Biotechnol.*, 2013, **163**(2), 243–249, DOI: **10.1016/j.jbiotec.2012.06.036**.

28 C. E. Ziegler, M. Graf, M. Nagaoka, H. Lehr and A. M. Goepferich, In Situ Forming iEDDA Hydrogels with Tunable Gelation Time Release High-Molecular Weight Proteins in a Controlled Manner Over an Extended Time, *Biomacromolecules*, 2021, **22**(8), 3223–3236, DOI: **10.1021/acs.biomac.1c00299**.

29 D. Kuzman, M. Bunc, M. Ravnik, F. Reiter, L. Žagar and M. Bončina, Long-Term Stability Predictions of Therapeutic Monoclonal Antibodies in Solution Using Arrhenius-Based Kinetics, *Sci. Rep.*, 2021, **11**, 20534, DOI: **10.1038/s41598-021-99875-9**.

30 L. Levintov and H. Vashisth, Role of Salt-Bridging Interactions in Recognition of Viral RNA by Arginine-Rich Peptides, *Biophys. J.*, 2021, **120**(22), 5060–5073, DOI: **10.1016/j.bpj.2021.10.007**.

31 X. Qian, J. Yin, S. Feng, S. Liu and Z. Zhu, Preparation and Characterization of Polyvinylpyrrolidone Films Containing Silver Sulfide Nanoparticles, *J. Mater. Chem.*, 2001, **11**(10), 2504–2506, DOI: **10.1039/B103708K**.

32 S. D. Buckel, P. F. Cottam, V. Simplaceanu and C. Ho, Formation of Intermolecular and Intramolecular Hydrogen Bonds in Histidine-Binding Protein J of Salmonella Typhimurium upon Binding L-Histidine. A Proton Nuclear Magnetic Resonance Study, *J. Mol. Biol.*, 1989, **208**(3), 477–489, DOI: **10.1016/0022-2836(89)90511-1**.

33 Y. Huan, S. Jung Park, K. C. Gupta, S.-Y. Park and I.-K. Kang, Slide Cover Glass Immobilized Liquid Crystal Microdroplets for Sensitive Detection of an IgG Antigen, *RSC Adv.*, 2017, **7**(60), 37675–37688, DOI: **10.1039/C7RA06386E**.

34 Y. He, S. Hong, M. Wang, J. Wang, A. M. A. El-Aty, J. Wang, A. Hacimuftuoglu, M. Khan and Y. She, Development of Fluorescent Lateral Flow Test Strips Based on an Electrospun Molecularly Imprinted Membrane for Detection of Triazophos Residues in Tap Water, *New J. Chem.*, 2020, **44**(15), 6026–6036, DOI: **10.1039/D0NJ00269K**.

35 R. Chari, K. Jerath, A. V. Badkar and D. S. Kalonia, Long- and Short-Range Electrostatic Interactions Affect the Rheology of Highly Concentrated Antibody Solutions, *Pharm. Res.*, 2009, **26**(12), 2607–2618, DOI: **10.1007/s11095-009-9975-2**.

36 T. Cloutier, C. Sudrik, N. Mody, H. A. Sathish and B. L. Trout, Molecular Computations of Preferential Interaction Coefficients of IgG1 Monoclonal Antibodies with Sorbitol, Sucrose, and Trehalose and the Impact of These Excipients on Aggregation and Viscosity, *Mol. Pharmaceutics*, 2019, **16**(8), 3657–3664, DOI: **10.1021/acs.molpharmaceut.9b00545**.

37 A. P. Minton, Recent Applications of Light Scattering Measurement in the Biological and Biopharmaceutical Sciences, *Anal. Biochem.*, 2016, **501**, 4–22, DOI: **10.1016/j.ab.2016.02.007**.
38 F. Chemat, H. Anjum, A. M. Shariff, P. Kumar and T. Murugesan, Thermal and Physical Properties of (Choline Chloride+urea+l-Arginine) Deep Eutectic Solvents, *J. Mol. Liq.*, 2016, **218**, 301–308, DOI: **10.1016/j.molliq.2016.02.062**.
39 M. Kunitz, Syneresis and Swelling of Gelatin, *J. Gen. Physiol.*, 1928, **12**(2), 289–312, DOI: **10.1085/jgp.12.2.289**.
40 H. J. M. Van Dijk, P. Walstra and J. Schenk, Theoretical and Experimental Study of One-Dimensional Syneresis of a Protein Gel, *Chem. Eng. J.*, 1984, **28**(3), B43–B50, DOI: **10.1016/0300-9467(84)85062-5**.
41 A. P. Constantinou, V. Nele, J. J. Doutch, J. S. Correia, R. V. Moiseev, M. Cihova, D. C. A. Gaboriau, J. Krell, V. V. Khutoryanskiy, M. M. Stevens and T. K. Georgiou, Investigation of the Thermogelation of a Promising Biocompatible ABC Triblock Terpolymer and Its Comparison with Pluronic F127, *Macromolecules*, 2022, **55**(5), 1783–1799, DOI: **10.1021/acs.macromol.1c02123**.
42 X.-L. Sun, P.-C. Tsai, R. Bhat, E. M. Bonder, B. Michniak-Kohn and A. Pietrangelo, Thermoresponsive Block Copolymer Micelles with Tunable Pyrrolidone-Based Polymer Cores: Structure/Property Correlations and Application as Drug Carriers, *J. Mater. Chem. B*, 2015, **3**(5), 814–823, DOI: **10.1039/C4TB01494D**.
43 H. Wei, X.-Z. Zhang, H. Cheng, W.-Q. Chen, S.-X. Cheng and R.-X. Zhuo, Self-Assembled Thermo- and pH Responsive Micelles of Poly(10-undecenoic acid-b-N-isopropylacrylamide) for Drug Delivery, *J. Controlled Release*, 2006, **116**(3), 266–274, DOI: **10.1016/j.jconrel.2006.08.018**.
44 H. Soleymani Abyaneh, M. R. Vakili, F. Zhang, P. Choi and A. Lavasanifar, Rational Design of Block Copolymer Micelles to Control Burst Drug Release at a Nanoscale Dimension, *Acta Biomater.*, 2015, **24**, 127–139, DOI: **10.1016/j.actbio.2015.06.017**.
45 T. A. Shmool, P. J. Woodhams, M. Leutzsch, A. D. Stephens, M. U. Gaimann, M. D. Mantle, G. S. Kaminski Schierle, C. F. van der Walle and J. A. Zeitler, Observation of High-Temperature Macromolecular Confinement in Lyophilised Protein Formulations Using Terahertz Spectroscopy, *Int. J. Pharm.: X*, 2019, **1**, 100022, DOI: **10.1016/j.ijpx.2019.100022**.
46 T. A. Shmool, P. J. Hooper, G. S. Kaminski Schierle, C. F. van der Walle and J. A. Zeitler, Terahertz Spectroscopy: An Investigation of the Structural Dynamics of Freeze-Dried Poly Lactic-co-glycolic Acid Microspheres, *Pharmaceutics*, 2019, **11**(6), 291, DOI: **10.3390/pharmaceutics11060291**.
47 D. Kumar Sahoo, S. Jena, J. Dutta, S. Chakrabarty and H. S. Biswal, Critical Assessment of the Interaction between DNA and Choline Amino Acid Ionic Liquids: Evidences of Multimodal Binding and Stability Enhancement, *ACS Cent. Sci.*, 2018, **4**(12), 1642–1651, DOI: **10.1021/acscentsci.8b00601**.
48 V. Andrushchenko and W. Pohle, Influence of the Hydrophobic Domain on the Self-Assembly and Hydrogen Bonding of Hydroxy-Amphiphiles, *Phys. Chem. Chem. Phys.*, 2019, **21**(21), 11242–11258, DOI: **10.1039/C9CP01475F**.
49 J. Tang, R. Mao, M. A. Tung and B. G. Swanson, Gelling Temperature, Gel Clarity and Texture of Gellan Gels Containing Fructose or Sucrose, *Carbohydr. Polym.*, 2001, **44**(3), 197–209, DOI: **10.1016/S0144-8617(00)00220-4**.
50 K. Nishinari and M. Watase, Effects of Sugars and Polyols on the Gel-Sol Transition of Kappa-Carrageenan Gels, *Thermochim. Acta*, 1992, **206**, 149–162, DOI: **10.1016/0040-6031(92)85293-5**.
51 G. Levy and T. W. Schwarz, The Effect Of Certain Additives On The Gel Point Of Methylcellulose, *J. Pharm. Sci.*, 1958, **47**(1), 44–46, DOI: **10.1002/jps.3030470113**.
52 N. L. Slack, P. Davidson, M. A. Chibbaro, C. Jeppesen, P. Eiselt, H. E. Warriner, H.-W. Schmidt, P. Pincus and C. R. Safinya, The Bridging Conformations of Double-End Anchored Polymer-Surfactants Destabilize a Hydrogel of Lipid Membranes, *J. Chem. Phys.*, 2001, **115**, 6252, DOI: **10.1063/1.1399061**.
53 P. Naranga and P. Venkatesu, Unravelling the Role of Polyols with Increasing Carbon Chain Length and OH Groups on the Phase Transition Behavior of PNIPAM, *New J. Chem.*, 2018, **42**(16), 13708–13717, DOI: **10.1039/C8NJ02510J**.
54 G. Bellavia, L. Paccou, Y. Guinet and A. Hédoux, How Does Glycerol Enhance the Bioprotective Properties of Trehalose? Insight from Protein–Solvent Dynamics, *J. Phys. Chem. B*, 2014, **118**(30), 8928–8934, DOI: **10.1021/jp500673b**.
55 M. Batens, T. A. Shmool, J. Massant, J. A. Zeitler and G. Van den Mooter, Advancing Predictions of Protein Stability in the Solid State, *Phys. Chem. Chem. Phys.*, 2020, **22**(30), 17247–17254, DOI: **10.1039/D0CP00341G**.
56 T. Senturk Parreidt, M. Schott, M. Schmid and K. Müller, Effect of Presence and Concentration of Plasticizers, Vegetable Oils, and Surfactants on the Properties of Sodium-Alginate-Based Edible Coatings, *Int. J. Mol. Sci.*, 2018, **19**(3), 742, DOI: **10.3390/ijms19030742**.
57 C. Olsson and J. Swenson, Structural Comparison between Sucrose and Trehalose in Aqueous Solution, *J. Phys. Chem. B*, 2020, **124**(15), 3074–3082, DOI: **10.1021/acs.jpcb.9b09701**.
58 T. Starciuc, B. Malfait, F. Danede, L. Paccou, Y. Guinet, N. T. Correia and A. Hedoux, Trehalose or Sucrose: Which of the Two Should be Used for Stabilizing Proteins in the Solid State? A Dilemma Investigated by In Situ Micro-Raman and Dielectric Relaxation Spectroscopies During and After Freeze-Drying, *J. Pharm. Sci.*, 2020, **109**(1), 496–504, DOI: **10.1016/j.xphs.2019.10.055**.